

# We are IntechOpen, the world's leading publisher of Open Access books Built by scientists, for scientists

## 4,800

Open access books available

## 122,000

International authors and editors

## 135M

Downloads

Our authors are among the

## 154

Countries delivered to

## TOP 1%

most cited scientists

## 12.2%

Contributors from top 500 universities

**WEB OF SCIENCE™**Selection of our books indexed in the Book Citation Index  
in Web of Science™ Core Collection (BKCI)

Interested in publishing with us?  
Contact [book.department@intechopen.com](mailto:book.department@intechopen.com)

Numbers displayed above are based on latest data collected.

For more information visit [www.intechopen.com](http://www.intechopen.com)

# Thermal Property Measurement of Al<sub>2</sub>O<sub>3</sub>-Water Nanofluids

Fei Duan  
*School of Mechanical and Aerospace Engineering, Nanyang Technological University  
Singapore*

## 1. Introduction

Fluids have been applied in the cooling in the most important industries including microelectronics, manufacturing, metrology, etc. With increasing thermal loads that require advances in cooling the new higher power output devices with faster speeds and smaller feature, the conventional heat transfer fluids, such as water, engine oil, ethylene glycol, etc., demonstrate the relative low heat transfer performance. The use of solid particles as an additive suspended in the base fluid is a potential alternative technique for the heat transfer enhancement, i.e. thermal conductivity of metallic or nonmetallic solids might have two orders of magnitude higher than the conventional fluids. The enhancement of thermal conductivity of conventional fluids with the suspension of solid particles, such as micrometer-sized particles, has been well known for more than 100 years (Choi, 1995). However, the conventional micrometer-sized particle liquid suspensions require high concentrations (>10%) of particles to achieve such an enhancement. Because they have the rheological and stability problems such as sedimentation, erosion, fouling, and pressure drop in flow channels, the fluids with the micrometer-sized particle have not been of interest for practical applications. The recent advance in materials technology has made it possible to produce nanometer-sized particles that can overcome these above problems. The innovative fluids suspended with nanometer-sized solid particles can change the transport and thermal properties of the base fluid, and make the fluid stable.

Modern nanotechnology can produce materials with average particle sizes below 50 nm. All solid nanoparticles with high thermal conductivity can be used as additives of nanofluids. These nanoparticles that have been usually used in the nanofluids include: metallic particles (Cu, Al, Fe, Au, Ag, etc.), and nonmetallic particles (Al<sub>2</sub>O<sub>3</sub>, CuO, Fe<sub>3</sub>O<sub>4</sub>, TiO<sub>2</sub>, SiC, carbon nanotube, etc.). The base media of nanofluids are usually water, oil, acetone, decene, ethylene glycol, etc. (Li et al., 2009). A 40% increase in thermal conductivity was found in the Cu oil-based nanofluids with 0.3% volume concentration, while the Al<sub>2</sub>O<sub>3</sub> water-based nanofluids exhibited a 29% enhancement of thermal conductivity for the 5% volume concentration nanofluids (Eastman et al., 1997).

The Al<sub>2</sub>O<sub>3</sub> nanoparticles were selected to prepare the water-based nanofluids in this study due to their chemical stability. Preparation of nanofluids is the key step in the use of nanoparticles for stable nanofluids. Two kinds of methods have been employed in producing nanofluids: the single-step method and the two-step method. The single-step method is a process combining the preparation of nanoparticles with the synthesis of nanofluids, for which the nanoparticles are directly prepared by the physical vapor deposition technique

or the liquid chemical method (Choi, 1995; Eastman et al., 1997). The processes of drying, storage, transportation, and dispersion of nanoparticles can be avoided, so the aggregation of nanoparticles is minimized and the stability of fluids is increased. But a disadvantage of the method is that only low vapor pressure fluids are compatible with the process. It limits the applications of the method. The two-step method for preparing nanofluids is a process by dispersing nanoparticles into base liquids. Eastman et al. (1997), Lee et al. (1999), and Wang et al. (1999) used this method to produce the  $\text{Al}_2\text{O}_3$  nanofluids. Nanoparticles used in the method are firstly produced as a dry powder by inert gas condensation, chemical vapor deposition, mechanical alloying, or the other suitable techniques before the nano-sized powder is then dispersed into a fluid in the second processing step. This step-by-step method isolates the preparation of the nanofluids from the preparation of nanoparticles. As a result, aggregation of nanoparticles may take place in both the steps, especially in the process of drying, storage, and transportation of nanoparticles. The aggregation would not only result in the settlement and clogging, but also affect the thermal properties. The techniques such as ultrasonic agitation or the addition of surfactant into the fluids are often used to minimize particle aggregation and improve dispersion behavior. Since nanopowder synthesis techniques have already been commercialized, there are potential economic advantages in using the two-step synthesis method. But an important problem that needs to be solved is the stabilization of the suspension to be prepared.

Nanofluids are a new class of solid-liquid composite materials consisting of solid nanoparticles, with sizes typically in the order of 1 - 100 nm, suspending in a heat transfer liquid. Nanofluids are expected to have superior properties compared to conventional heat transfer fluids. The much larger relative surface area of nanoparticles should not only significantly improve heat transfer capabilities (Xie et al., 2001), but also increase the stability of the suspensions. In addition, nanofluids can improve abrasion-related properties as compared to the conventional solid/fluid mixtures. Successful applications of nanofluids would support the current trend toward component miniaturization by enabling the design of smaller but higher-power heat exchanger systems (Kebblinski et al., 2005). The thermal properties including thermal conductivity, viscosity, and surface tension have been investigated.

### 1.1 Thermal conductivity of nanofluids

Since the model reported by Maxwell (1892), the classical models have been derived by Hamilton & Crosser (1962), Bruggeman (1935), and Xuan & Li (2000) for predicting the effective thermal conductivity of a continuum mixture with the assumed well-dispersed solid particles in the base fluid. The Maxwell model was developed to determine the effective thermal conductivity of liquid-solid suspensions for a low volumetric concentration of spherical particles. This model is applicable to statistically homogeneous low volume fraction liquid-solid suspensions with randomly dispersed and uniform spherical particles in size. For non-spherical particles, the thermal conductivity of the nanofluids depends not only on the volume fraction of the particles, but also on the shape of the particles. Hamilton & Crosser (1962) modified the Maxwell model to determine the effective thermal conductivity of nonspherical particles by applying a shape factor for the effective thermal conductivity of two-component mixtures. The Hamilton-Crosser model considers the nanoparticle aggregation. For spherical particles, the Hamilton-Crosser model reduces to the Maxwell model. In the Bruggeman model, the mean field approach is used to analyze the interactions among the randomly distributed particles (Bruggeman, 1935). The model by Xuan & Li (2000) is not specified for any particular shape of particles. However, the classical

models were found to be unable to predict the anomalously high thermal conductivity of nanofluids. This might be because these models do not include the effects of particle size, interfacial layer at the particle/liquid interface, and the Brownian motion of particles (Jang & Choi, 2004; Keblinski et al., 2002; Wang et al., 1999; Yu & Choi, 2003). Recently, Yu & Choi (2003) proposed a modified Maxwell model to account for the effect of the nano-layer by replacing the thermal conductivity of solid particles with the modified thermal conductivity of particles, which is based on the so called effective medium theory (Schwartz et al., 1995). The model can predict the presence of thin nano-layers less than 10 nm in thickness. Yu & Choi (2004) proposed a modified Hamilton-Crosser model to include the particle-liquid interfacial layer for nonspherical particles. The model can predict the thermal conductivity of the carbon nanotube-in-oil nanofluids reasonably well. However, it fails to predict the nonlinear behavior of the effective thermal conductivity of general oxide and metal based nanofluids. Xue (2003) presented a model for the effective thermal conductivity of nanofluids considering the effect of the interface between the solid particles and the base fluid based on the Maxwell model and the average polarization theory. Xue (2003) demonstrated that the model predictions were in a good agreement with the experiments of the nanotube oil-based nanofluids at high thermal conductivity and nonlinearity. However, Yu & Choi (2004) found that the predicted values from the model by Xue are inaccurate by using two incorrect parameters, as same as the finding of Kim et al. (2004). Xue & Xu (2005) obtained an equation for the effective thermal conductivity based on the Bruggeman model (Bruggeman, 1935). The equation takes account of the effect of interfacial shells by replacing the thermal conductivity of nanoparticles with the assumed value of the "complex nanoparticles", which introduces interfacial shells between the nanoparticles and the base fluids. The model can explain the size dependence of the thermal conductivity of nanofluids (Xuan & Li, 2000). Xie et al. (2001) considered the interfacial nano-layer with the linear thermal conductivity distribution and proposed an effective thermal conductivity model to account for the effects of nano-layer thickness, nanoparticles size, volume fraction, and thermal conductivities of fluids, and nanoparticles. They claimed that the calculated values could agree well with some available experimental data.

Temperature is one of the important factors influencing the thermal conductivity of nanofluids (Das et al., 2003; Li & Peterson, 2006; Yang & Han, 2006). Xuan et al. (2003) considered the Brownian motion of suspended nanoparticles on the basis of the Maxwell model. The prediction from the model is in an agreement with the experiment results, especially when the effect of nanoparticle aggregation is taken into account. But the model may be not accurate for the second term in the equation. Wang et al. (2003) proposed a fractal model for predicting the thermal conductivity of nanofluids based on the effective medium approximation and the fractal theory, developed firstly by Mandelbrot (1982). It can describe the disorder and stochastic process of clustering and polarization of nanoparticles within the mesoscale limit. A comprehensive model considering a large enhancement of thermal conductivity in nanofluids and its strong temperature dependence was deduced from the Stokes-Einstein formula by Kumar et al. (2004). The thermal conductivity enhancement takes into account of the Brownian motion of the particles. However, the validity of the model in the molecular size regime has to be explored and it may not be suitable for a large concentration of the particles where interactions of particles become important. Bhattacharya et al. (2004) developed a technique to compute the effective thermal conductivity of a nanofluid using the Brownian motion simulation. They combined the liquid conductivity and particle conductivity. The model showed a good agreement of the thermal conductivity of nanofluids. Jang & Choi (2004) combined four modes of energy transport in the nanofluids, collision between base fluid molecules, thermal diffusion of nanoparticles in fluids, collision between nanoparticles

due to the Brownian motion, and thermal interaction of dynamic nanoparticles with the base fluid molecules in their model, which considered the effects of concentration, temperature, and particle size. The predictions from this model agree with the experimental data of Lee et al. (1999) and Eastman et al. (2001). However, it may not be suitable in the high temperature since the Brownian motion effect was neglected. Prasher et al. (2005) proposed that the convection caused by the Brownian motion of nanoparticles is primarily responsible for the enhancement in the effective thermal conductivity of nanofluids. By introducing a general correlation for the heat transfer coefficient, they modified the Maxwell model by including the convection of the liquid near the particles due to the Brownian motion. The result showed that the model matched well with the experimental data under different fluid temperature in a certain range. A model for nanofluids, which takes account the effects of particle size, particle volume fraction and temperature dependence as well as properties of the base fluid and the particle subject to the Brownian motion, developed by Koo & Kleinstreuer (2004).

Although many models have been proposed, no theoretical models are available for predicting the thermal conductivity of nanofluids universally up to now. More experimental data are required. Such data should include more studies of the effects of size and shape of the nanoparticles, the interfacial contact resistance between nanoparticles and base fluids, the temperature dependence, the effect of the Brownian motion, or the effect of clustering of particles.

Experimental works have been reported on the thermal conductivity of nanofluids. The main techniques are the transient hot wire (THW) method (Kestin & Wakeham, 1978), the temperature oscillation technique (Wang et al., 1999), and the steady-state parallel-plate method (Das et al., 2003). Among them, the THW method has been used most extensively. Since most nanofluids are electrically conductive, a modified hot-wire cell with an electrical system was proposed by Nagasaka & Nagashima (1981). The advantage of the method is its almost complete elimination of the effect of natural convection. The measuring principle of the THW technique is based on the calculation of the transient temperature field around a thin hot wire as a line source. A constant current is supplied to the wire to raise its temperature. The heat dissipated in the wire increases the temperature of the wire as well as that of the nanofluids. This temperature rise depends on the thermal conductivity of the nanofluids in which the hot wire is at the center. Therefore, the thermal conductivity value of the fluid can be determined. The oscillation method was proposed by Roetzel et al. (1990) and further developed by Czarnetzki & Roetzel (1995). In principle, the thermal diffusivity of a fluid can be measured very accurately by considering amplitude attenuating of thermal oscillation from the boundary to the center of the fluid. However, for direct measurement of thermal conductivity one has to consider the influence of the reference materials as well. Since the defects of the reference materials might bring out the uncertainty in the thermal conductivity measurement, a direct evaluation of the thermal conductivity of the fluid is less accurate. The apparatus for the steady-state parallel-plate method can be constructed on the basis of the design by Challoner & Powell (1956). The steady-state parallel-plate method needs to measure the temperature increase accurately in each thermocouple (Das et al., 2003). The difference in temperature readings needs to be minimized when the thermocouples are at the same temperature. In this method, it has to follow the assumption that there is no heat loss from the fluid to the surrounding. As a result, guard heaters would be applied to maintain a constant temperature in the fluid. However, it is challenging to control the conditions in which no heat radiated to the surrounding from the fluid. Thus, the THW method was selected for this study.



## 1.2 Viscosity of nanofluids

Viscosity of nanofluids is an important parameter in the fluid transporting. However, the data collected showed that no theoretical models (Batchelor, 1977; Brinkman, 1952; Einstein, 1906; Frankel & Acrivos, 1967; Graham, 1981; Lundgren, 1967) succeed in predicting the viscosity of nanofluids accurately until now. A few theoretical models were used to estimate particle suspension viscosities. Almost all the formulae were derived from the pioneering work of Einstein (1906), which is based on the assumption of a linearly viscous fluid containing the dilute, suspended, and spherical particles. The Einstein formula is found to be valid for relatively low particle volume fractions less than 0.01. Beyond this value, it underestimates the effective viscosity of the mixture. Later, many works have been devoted to the "correction" of his formula. Brinkman (1952) has extended the Einstein formula for use with moderate particle concentration. Lundgren (1967) proposed an equation under the form of a Taylor series. Batchelor (1977) considered the effect of the Brownian motion of particles on the bulk stress of an approximately isotropic suspension of rigid and spherical particles. Graham (1981) generalized the work of Frankel & Acrivos (1967), but the correlation was presented for low concentrations. Almost no model mentioned could predict the viscosity of nanofluids in a wide range of nanoparticle volume fraction so far. According to these correlations the effective viscosity depends only on the viscosity of the base fluid and the concentration of the particles, whereas the experimental studies show that the temperature, the particle diameter, and the kind of nanoparticle can also affect the effective viscosity of a nanofluid. A good understanding of the rheological properties and flow behavior of nanofluids is necessary before nanofluids can be commercialized in the heat transfer applications. These factors influencing the viscosity include concentration, size of nanoparticles, temperature of nanofluids, shear rate, etc. Thus, more thorough investigations should be carried out on the viscosity of nanofluids.

In the measurement, the rotational rheometer, the piston-type rheometer, and the capillary viscometer are the most popular tools used to measure the viscosity of nanofluids. Rotational rheometers use the method that the torque required to turn an object in a fluid is a function of the viscosity (Chandrasekar et al., 2010). The relative rotation determines the shear stress under different rates. The advantage of this type of measurement is it is not affected by the flow rate of the fluids. The operation is simple and high repeatable. The piston type rheometer is based on the Couette flow inside a cylindrical chamber (Nguyen et al., 2007). It composes the magnetic coils installed inside a sensor body. These coils are used to generate a magnetically-induced force on a cylindrical piston that moves back and forth over a very small distance, imposing shear stress on the liquid. By powering the coils with a constant force alternatively, the elapsed time corresponding to a round trip of the piston can then be measured. Since the measurement of the piston motion is in two directions, variations due to gravity or flow forces are minimized. Because of the very small mass of the piston, the induced magnetic force would exceed any disturbances due to vibrations. However, the piston type viscometer is that the duration of the heating phase necessary to raise the fluid sample temperature is relative long, especially under the elevated temperature condition, some base fluids may be evaporated. The capillary viscometer is introduced in U-shaped arms (Li et al., 2007). The capillary viscometer is submerged in a glass water tank. A water tank is maintained at a prescribed constant temperature for the capillary viscometer by the water circulation. The vertical angle of the viscometer is accurately controlled with a special tripod. Li et al. (2007) pointed out that the capillary tube diameter may influence the apparent viscosity and result in inaccurate in the nanofluids at higher nanoparticle mass fractions, especially at a lower temperature. In addition, nanoparticles might stain at the inner wall of

the bore. Because of the narrow diameter, cleaning is difficult if the nanoparticles are left. In our study, we adopted the rotational rheometer to measure the viscosity of nanofluids because of its simplicity and repeatability.

### 1.3 Surface tension of nanofluids

Interfacial properties such as surface tension play an important role for the fluids having a free surface, however, the studies of the interfacial properties of nanofluids are limited. An understanding of nanofluid properties is essential so that we can optimize the usage of nanofluids and understand their limitations. The temperature dependence of surface tension of the liquid is crucial in the bubble or droplet formation. Wasan & Nikolov (2003) studied the spreading of nanofluids on solid surfaces and found that the existence of nanoparticles near the liquid/solid contact line can improve its spreading. Vafaei et al. (2009) investigated the effects of size and concentration of nanoparticles on the effective gas-liquid surface tension of the aqueous solutions of the bismuth telluride nanoparticles. Kumar & Milanova (2009) found that the single-walled carbon nanotube suspensions in a boiling environment can extend the saturated boiling regime and postpone catastrophic failure of the materials even further than that previously reported if the surface tension of the nanofluids is carefully controlled. The surface tension of a liquid strongly depends on the presence of contaminants or dispersion agents such as surfactants.

Pendant droplet analysis is a convenient way to measure surface tension of fluids. It is assumed that the droplet is symmetric and the drop is not in motion. The advantage of the technique is that the calibration is straightforward, only based on the optical magnification. This can lead to a high accuracy. Another advantage is that the cleanliness requirement is not high. Surface tension is determined by fitting the shape of the droplet to the Young-Laplace equation which relates surface tension to droplet shape. Pantzali et al. (2009) used the pendant droplet method to measure the surface tension of the CuO water-based nanofluids. The other common method to measure surface tension is the capillary method (Golubovic et al., 2009). The main component of the device is a capillary tube in which the liquids would show a significant rise with a meniscus due to the surface tension in order to balance the gravity force. The disadvantage of the capillary method is that cleaning is difficult if the nanoparticles are left in the small diameter capillary. Thus, the pendant drop technique was selected in this study.

In sum, the reported thermal property measurement are scattered, and lack of agreement with the models. It might be due to various factors such as the measuring technique, particle size, base fluid, volume fraction of nanoparticles in fluids, temperature, etc. The lack of reliable experimental data is one of the main reasons for no universal theoretical or empirical models. Therefore, we investigated the thermal properties of the Al<sub>2</sub>O<sub>3</sub> water-based nanofluids. The thermal conductivity, viscosity, and surface tension were measured. The effects of particle volume fraction, temperature and particle size were discussed at the end of experiments.

## 2. Experimental procedure

### 2.1 Preparation of Al<sub>2</sub>O<sub>3</sub> nanofluids

As discussed by Kwek et al. (2010), different sizes of the Al<sub>2</sub>O<sub>3</sub> nanoparticles and the surfactant, Cetyltrimethylammonium Bromide (CTAB), were purchased from Sigma Nanoamor and Aldrich respectively. During the experiments, we dispersed the Al<sub>2</sub>O<sub>3</sub> nanoparticles with an average diameter of 25 nm and particle density of 3.7 g/cm<sup>3</sup> into 100

ml of the de-ionized water to prepare the different volume concentrations (1%, 2%, 3%, 4%, and 5%). Oxide-particle volume concentrations are normally below 5% in order to maintain moderate viscosity increases. To investigate the particle size effect on the thermal conductivity and viscosity, additional four sets of nanofluids each with a constant volume concentration of 5% but with different particle sizes (10 nm, 35 nm, 80 nm and 150 nm) were prepared. Sample preparation is carried out by using a sensitive mass balance with an accuracy of 0.1 mg. The volume fraction of the powder is calculated from the weight of dry powder using the density provided by the supplier and the total volume of the suspension.

$$\text{vol}\% = \frac{m/\rho}{100\text{ml}_{\text{water}} + m/\rho} \quad (1)$$

where  $m$  and  $\rho$  are the mass and density of the Al<sub>2</sub>O<sub>3</sub> nanoparticles respectively.

The surfactant, CTAB with the density is 1.3115 g/cm<sup>3</sup> at volume percentage of around 0.01-0.02 can stabilize the nanofluids (Sakamoto et al., 2002). The amount of 0.01 vol % CTAB was added into the Al<sub>2</sub>O<sub>3</sub> water-based nanofluids to keep the nanoparticles well dispersed in the base fluid, water.

The nanofluid was then stirred by a magnetic stirrer for 8 hours before undergoing ultrasonicfication process (Fisher Scientific Model 500) for one and a half hours. This is to ensure uniform dispersion of nanoparticles and also to prevent the nanoparticles from the aggregation in the nanofluids.

## 2.2 Thermal conductivity measurement of Al<sub>2</sub>O<sub>3</sub> nanofluids

In the study, we adopted the THW technique for measuring thermal conductivity, as shown in Fig. 1. The setup consists of a direct current (DC) power supply, a Wheatstone bridge

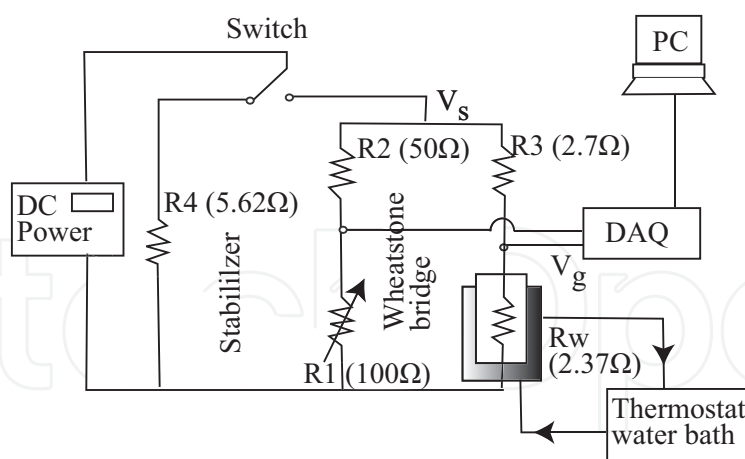


Fig. 1. Schematics of the THW setup (Kwek et al., 2010).

circuit, and a thin platinum wire surrounded by a circular nanofluid container, which is maintained by a thermostat bath. The DC power supply provides a constant voltage source to the Wheatstone bridge circuit at a constant rate to allow a uniform increment of temperature with respect to time. As the resistors used in this experiment have low values of resistance,  $V_s$  is adjusted to a value of between 0 to 2.5V. A data acquisition unit (Yokogawa Electric Corporation, DaqMaster MW100) is applied to capture the readings, recorded in a computer. The voltage supplied by the stabilizer, the voltage supplied in the Wheatstone circuit, the



voltage for the platinum wire and the voltage across bridge ( $V_g$ ) can be monitored during the experiments. The main experimental cell is a part of the Wheatstone bridge circuit since the wire is used as one arm of the bridge circuit. Teflon spray is used for coating a platinum (Pt) wire to act as an electric insulation because the  $\text{Al}_2\text{O}_3$  nanofluids are electrically conductive. The Pt wire has good resistance as a function of temperature over a wide temperature range. The resistance-temperature coefficient of the Pt wire is  $0.0039092 \text{ }^\circ\text{C}$  (Bentley, 1984). The Pt wire of  $100 \text{ }\mu\text{m}$  in diameter and  $180 \text{ mm}$  in length was used in the hot-wire cell whose electric resistance was measured. The dimensions of the nanofluid container are chosen to be sufficiently large to be considered as infinite in comparison with the diameter of the Pt wire. The volume and diameter of the nanofluid container are  $100 \text{ ml}$  and  $30 \text{ mm}$  respectively.

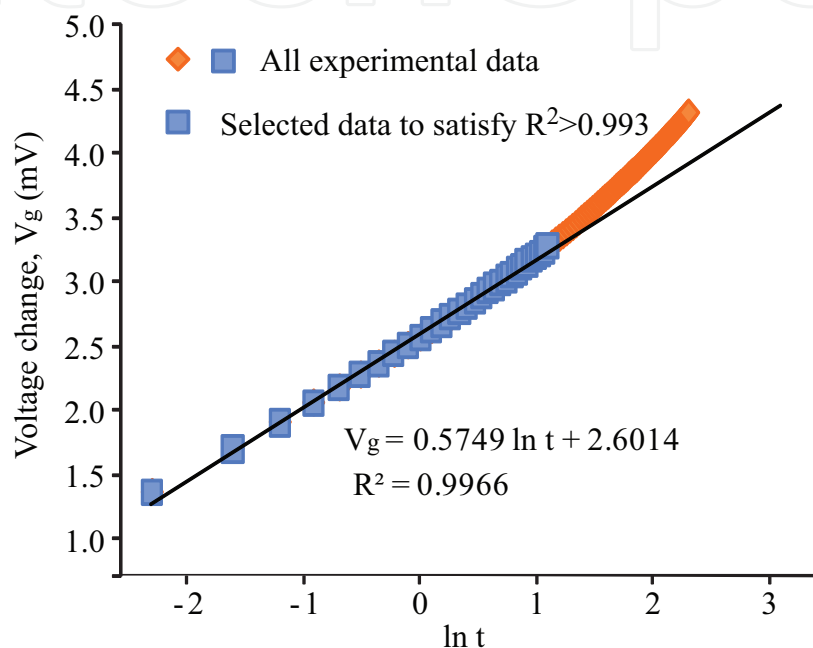


Fig. 2.  $V_g$  as a function of ( $\ln t$ ) with the linear fitting curve.

To investigate the effect of temperature from  $15$  to  $55 \text{ }^\circ\text{C}$  on the thermal conductivities of the nanofluids, the nanofluid container was enclosed with an acrylic container connected to a thermostat bath. Different temperatures of nanofluids can be reached during the measurement process. The nanofluid temperature was monitored with a thermocouple. In the measurement of the thermal conductivity of the  $\text{Al}_2\text{O}_3$  nanofluids, the cylindrical shaped nanofluid container was filled with  $100 \text{ ml}$  of the  $\text{Al}_2\text{O}_3$  water-based nanofluid. The required temperature was set at the thermostat to maintain a uniform temperature in the nanofluid. Then the DC power source was switched on with the input voltage ( $V_s$ ) being adjusted to  $0.5 \text{ V}$  while the switch in the circuit remained on the stabilizer resistor ( $R_4$  in Fig. 1) circuit. Thereafter, the switch was turned to the Wheatstone bridge circuit and  $V_g$  (Fig. 1) was balanced by adjusting manually the variable resistor in circuit. Once there was no voltage change, the circuit was considered as being balanced. Again, it was switched back to the stabilizer resistor circuit and input voltage  $V_s$  was then set to the desired value of  $2.0 \text{ V}$  before the switch was set back to the Wheatstone bridge circuit. The unbalanced voltage change ( $V_g$ ) occurring in the hot wire was recorded for  $10$  seconds in the computer via a data acquisition unit. The input voltage to the circuit was also recorded for each run. This measured unbalanced voltage over the natural logarithm of time was plotted in Fig. 2 by using Equation (2) (Kwek et al., 2010). The thermal conductivity is then calculated from the

slope and intersect.

$$V_g = \frac{R_3}{(R_3 + R_w)^2} (\beta R_w) \frac{V_s q}{4\pi k} \left( \ln t + \ln \frac{4\alpha}{a^2 C} \right) \quad (2)$$

where  $V_g$  can be obtained directly from the Wheatstone bridge circuit,  $V_s$  is the voltage supplied,  $R_w$  is the known resistance of the Pt wire,  $R_3$  is the resistance along same branch of Wheatstone circuit,  $q$  is the heat rate per unit length,  $\alpha$  is the thermal diffusivity of the surrounding medium,  $\beta$  is the resistance-temperature coefficient of the wire,  $k$  is the thermal conductivity to be determined, and  $C = \exp(0.5772)$ .

Figure 2 shows a sample of the unbalanced voltage ( $V_g$ ) as a function of the natural logarithm of time. The best fitting with  $R_2 > 0.993$  was applied to determine the thermal conductivity. The average thermal conductivity was then determined.

Before the experiments of nanofluids, the THW setup was calibrated with the de-ionized water, the procedure was as same as the experimental process for measuring the thermal conductivity of nanofluids. The calibration showed that the accuracy of the measured thermal conductivity values is in  $\pm 2\%$  from the documental data.

### 2.3 Viscosity measurement of Al<sub>2</sub>O<sub>3</sub> nanofluids

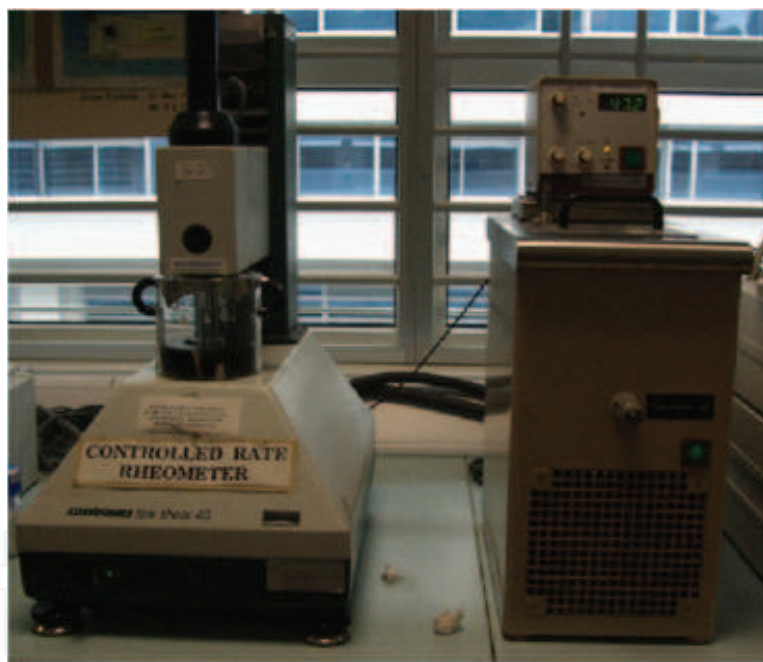


Fig. 3. The image of the controlled shear rate rheometer (Contraves LS 40).

As shown in Fig. 3, the controlled shear rate rheometer (Contraves LS 40) was applied to measure the viscosity of the Al<sub>2</sub>O<sub>3</sub> nanofluids. The rheometer has a cup and bob geometry. The bob is connected to the spindle drive while the cup is mounted onto the rheometer. As the cup is rotated, the viscous drag of the fluid against the spindle is measured by the deflection of the torsion wire. The cup and bob geometry requires a sample volume of around 5 ml, hence, the temperature equilibrium can be achieved quickly within 5 minutes. The spindle type and speed combination would produce satisfactory results when the applied torque is up to 100% of the maximum permissible torque. In the measurement, the cup was placed onto the rheometer while the bob was inserted into the top shaft. The nanofluids were then transferred to the cup in preventing any bubbles forming. Afterwards, the bob was lowered down until

it was completely inserted into the cup and immersed in the nanofluids. The lever knob was then adjusted until the bob and cup were concentric. After the measuring settings such as the minimum and maximum shear rates were set, the experiment was run. The viscosity as a function of the shear rate was plotted.

For the temperature effect, the rheological property of the nanofluids was measured by the viscometer with the thermostat, which controls temperature in Fig. 3. The viscosity measurement was started at 15 °C, and temperature was gradually increased to 55 °C at an interval of 10 °C. The nanofluid temperature was also measured by using a thermocouple. All the viscosity measurements were recorded at steady state conditions.

Before the measurement of nanofluids, the viscometer was calibrated with the de-ionized water, having an error within  $\pm 1\%$ .

#### 2.4 Surface tension measurement of Al<sub>2</sub>O<sub>3</sub> nanofluids

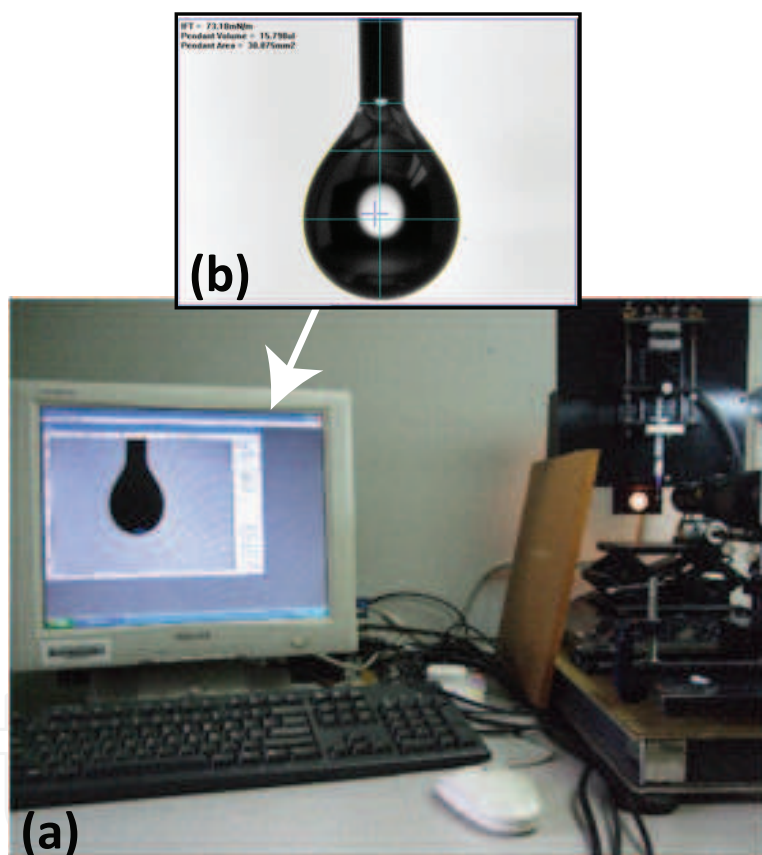


Fig. 4. Surface tension measurement for Al<sub>2</sub>O<sub>3</sub> water-based nanofluids, (a) FTA 200 system; (b) a pendant droplet of the fluid for measurement.

The surface tension of the Al<sub>2</sub>O<sub>3</sub> water-based nanofluids under different volume concentrations was measured with First Ten Angstroms (FTA) 200, illustrated in Fig. 4a. The precision syringe pumps (KD Scientific Inc., USA) was used to drive the Al<sub>2</sub>O<sub>3</sub> water-based nanofluids to form a pendant droplet as shown in Fig. 4b. An epi-fluorescent inverted microscope with a filter set (Nikon B-2A, excitation filter for 450 - 490 nm, dichroic mirror for 505 nm and emission filter for 520 nm) was used to monitor the hanging droplet. A sensitive interline transfer CCD camera (HiSense MKII, Dantec Dynamics, Denmark) was employed for recording the droplet shape.

In the experiments, the Al<sub>2</sub>O<sub>3</sub> nanofluids with a certain volume concentration were filled into the syringe, which was held at the loading platform as shown in Fig. 4a. Once a pendant nanofluid droplet was formed, the image of droplet was taken. The surface tension, the droplet volume, and the surface area were then computed.

The calibration was conducted with the de-ionized water before the surface tension of nanofluid was measured. It was found that the surface tension of pure water was  $72.93 \pm 1.01$  mN/m at room temperature. The value is very close to the standard value at 71.97 mN/m (Vargaftik et al., 1983).

### 3. Results and discussion

#### 3.1 Thermal conductivity of Al<sub>2</sub>O<sub>3</sub> nanofluids

##### 3.1.1 Effect of volume concentration on thermal conductivity

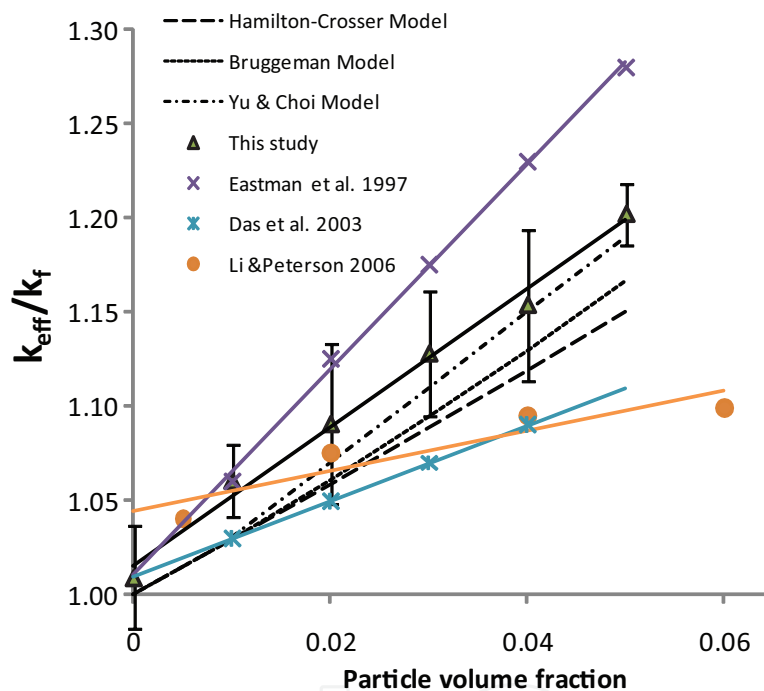


Fig. 5. Thermal conductivity enhancement as a function of volume concentrations of Al<sub>2</sub>O<sub>3</sub> water-based nanofluids at 25 °C.

Each of the experimental data represents the average of six measurements at a specific concentration under room temperature. As shown in Fig. 5, the effective thermal conductivity ratio ( $k_{eff}/k_f$ ) of the nanofluids is plotted as a function of nanoparticle volume fraction for a series of the Al<sub>2</sub>O<sub>3</sub> nanofluids prepared from 25 nm Al<sub>2</sub>O<sub>3</sub> powders and measured at 25 °C.  $k_{eff}$  is the measured thermal conductivity of the nanofluids and  $k_f$  is the thermal conductivity of pure water. Figure 5 also illustrates the data reported by Eastman et al. (1997) (33 nm), Das et al. (2003) (38.4 nm), Li & Peterson (2006) (36 nm), and the prediction from the Hamilton-Crosser model (Hamilton & Crosser, 1962), Bruggeman model (Bruggeman, 1935), and the modified model by Yu & Choi (2003). Direct quantitative comparisons are not possible in this case as the particle size used by the other researchers differs from this experimental results (25 nm). It can be noted that the previous experimental results, the predicted thermal conductivity, and the measured values in the study increase with an

increase of nanoparticle concentration in a distinct linear fashion. However, the slopes are not same. From our experimental results, it is found that a small volume percentage at 1 - 5% addition of the  $\text{Al}_2\text{O}_3$  nanoparticles in the water significantly increases the effective thermal conductivity of the  $\text{Al}_2\text{O}_3$  water-based nanofluids by 6 to 20% respectively. If we disregard the minor differences in the particles size, clear discrepancies were found between the previous experimental data and ours on the amount of enhancement in Fig. 5. This difference may be caused by the various factors such as the different particle preparation, the particle source, or even the measurement technique. Up to now, there are no standard guidelines on the preparation of nanofluids such as the amount and type of surfactant added, the time duration for ultrasonification process, the measurement method and procedures, and the size and shape of nanoparticles in use. All these might add up to account for the difference in the experimental data.

By comparing the percentage difference in the effective thermal conductivity ratio with the measured values, our data are more consistent with the predicted values of the Yu & Choi correlation than those of the other correlations, especially at a high volume concentration where the percentage difference at 0.04 and 0.05 volume fraction is around 0.4 % and 1 % respectively. Thus, the conventional models underestimate the thermal conductivity enhancement when compared against the measured values. The reason may be that the present proposed models did not take into account the additional mechanisms such as the interfacial layer, the Brownian motion, the size and the shape of nanoparticles, and the nanoparticle aggregation. At this stage, most of these aforementioned mechanisms are neither well established nor well understood. Therefore, more experimental works are required before the concrete conclusions can be inferred from the thermal behavior of nanofluids.

### 3.1.2 Effect of temperature on thermal conductivity

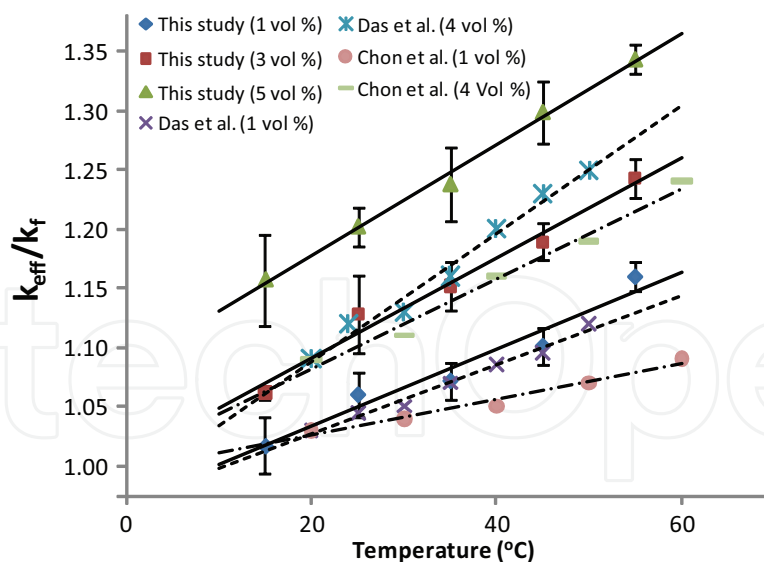


Fig. 6. Temperature dependence of thermal conductivity enhancement for the  $\text{Al}_2\text{O}_3$  water-based nanofluids.

The effective thermal conductivity ratio ( $k_{eff}/k_f$ ) is expressed with a reference of the measured value of water at the related temperatures. The measurement was made for the  $\text{Al}_2\text{O}_3$  water-based nanofluids with the given particle concentrations at different temperatures. Figure 6 shows the enhancement of thermal conductivity of  $\text{Al}_2\text{O}_3$  nanofluids with temperature. There is a considerable increase in the enhancement from 15 to 55 °C in



the nanofluids of 1 vol %, 3 vol %, and 5 vol %. With 1 vol % particles at about 15 °C, the enhancement is only about 1.7 %, but about 16 % at 55 °C. The present measurement shows that a higher enhancement can be achieved in the nanofluid having small volume ratio of nanoparticles in the fluids at a higher temperature. The measurement of 3 vol % and 5 vol % nanofluids shown in Fig. 6 demonstrates the enhancement goes from 6 % to 24 % and 15 % to 34 % respectively as a function of temperature from 15 to 55 °C. The average rate of enhancement in these cases is higher compared with that of 1 vol % nanofluids. The increasing slope of the fitted line of the 1 vol %, 3 vol %, or 5 vol % nanofluids has a gradient of 0.003575, 0.0045 or 0.00475 respectively. Thus it can be said that the enhancement of thermal conductivity with increases of temperature depends on the concentration of nanoparticles. The above trends are also explained by the experimental results of Das et al. (2003) (38.4 nm) and Chon et al. (2005) (47 nm) in Fig. 6. From the data of Das et al., the increasing rates are 0.002 and 0.005 for 1 vol % and 4 vol %, whereas the results of Chon et al. show the increasing rates of 0.001 and 0.003 for the nanofluids at 1 vol % and 4 vol %. The increasing trends observed are quite similar.

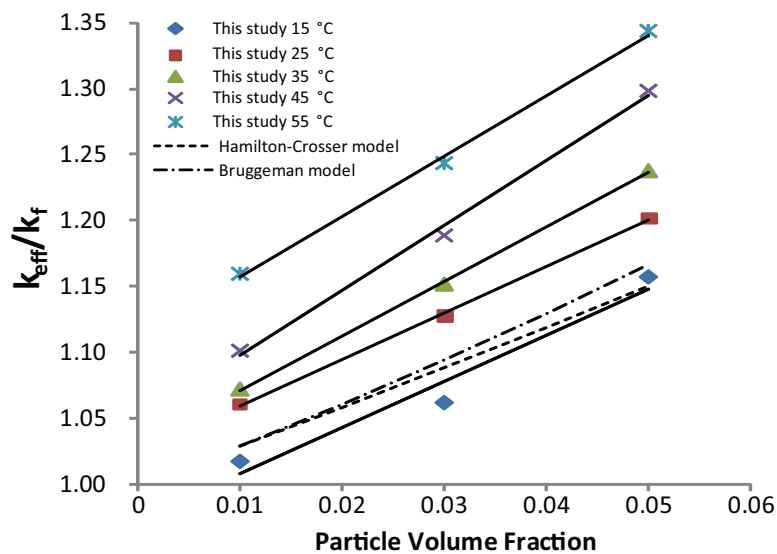


Fig. 7. Enhancement of thermal conductivity of the Al<sub>2</sub>O<sub>3</sub> water-based nanofluids against particles concentration and comparison with models.

Figure 7 shows that there is a close agreement between the measured thermal conductivity and the Hamilton-Crosser and the Bruggeman models at 15 °C. However, this agreement is only at the low temperature. At higher temperature, the experiments of the Al<sub>2</sub>O<sub>3</sub> water-based nanofluids disagree with the models. It is suggested that the present models cannot reflect on the effective conductivity with temperature. Das et al. (2003) stated that the main mechanism of the thermal conductivity enhancement in nanofluids can be thought as the stochastic motion of nanoparticles, and that the Brownian motion would depend on the fluid temperature. This enhancement in our experiments can be supported by the results of Das et al. (2003) and Chon et al. (2005). Their data have the maximum enhancements of 25 % and 19 % for 4 vol % at 55 °C whereas the Hamilton-Crosser model (Hamilton & Crosser, 1962) and the Bruggeman model (Bruggeman, 1935) predict only 12 % and 13 %, regardless of the temperature effect. At the low temperature, the Brownian motion was less significant. Thus the present results indicate that it is possible to have a threshold temperature at which the effective thermal conductivity of nanofluids starts deviating from that of the usual suspension and the enhancement through the stochastic motion of the particles starts

dominating. The measurement of the thermal conductivity with the given concentrations at the different temperatures in Fig. 7 indicates the necessity for a better theoretical model for the entire range of temperature.

### 3.1.3 Effects of particle size on thermal conductivity

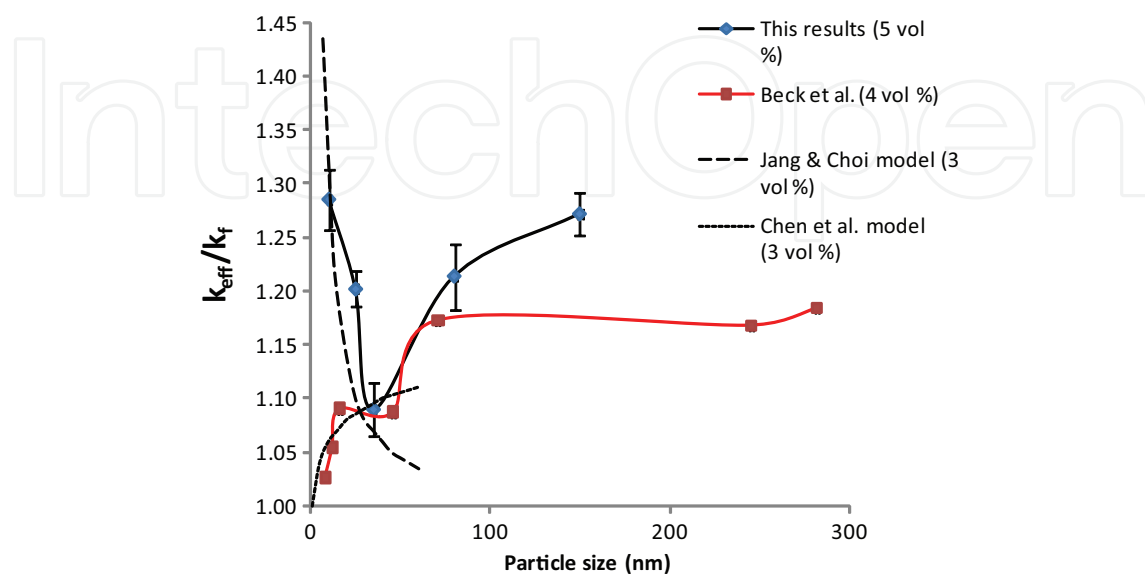


Fig. 8. Effect of diameter of nanoparticle on effective thermal conductivity of the  $\text{Al}_2\text{O}_3$  water-based nanofluids.

As shown in Fig. 8, the experimental data in the study are compared with the predictions from the thermal conductivity model by Jang & Choi (2004), and a good agreement was found for 10 nm, 25 nm and 35 nm  $\text{Al}_2\text{O}_3$  water-based nanofluids. Our experimental data indicate that the effective thermal conductivity decreases quickly with the decreasing size of nanoparticles from 10 nm to 35 nm, however as the nanoparticle size increases, the thermal conductivity deviates from the Jang & Choi model. As the nanoparticle diameter is reduced, the effective thermal conductivity of nanofluids becomes larger. Jang & Choi (2004) explained that this phenomenon is based on the Brownian motion, and that the smaller nanoparticles in average might produce a higher velocity of the Brownian motion in the fluid. As a result, the heat transfer by the convection would be enhanced, the effective thermal conductivity of nanofluids increases. However, if the particles approach the micrometer size, they might not remain well suspended in the base fluid. Thus, large microparticles do not have the Brownian motion any more, and there would be no enhancement of the effective thermal conductivity. Our experimental results for the nanofluids with the 80 nm and 150 nm  $\text{Al}_2\text{O}_3$  nanoparticles did not show a similar trend as described in the model of Jang & Choi (2004). Instead our experimental data shows that the thermal conductivity of the  $\text{Al}_2\text{O}_3$  nanofluids increases as the particle size increases above 35 nm, similar to the data of Beck et al. (2009) above 50 nm. When the particles become larger, it can be better explained by the model of Chen (1996),

$$k_p = k_{bulk} \frac{0.75d_p/l_p}{0.75d_p/l_p + 1} \quad (3)$$

where  $k_p$ ,  $d_p$ ,  $l_p$  and  $k_{bulk}$  are the thermal conductivity of nanoparticle, the characteristic length of nanoparticles, the mean free path of nanoparticle, and the thermal conductivity of bulk materials respectively. The correlation of Chen (1996) is built on solving the Boltzmann

transport equation. The solution approaches the prediction of the Fourier law when the particle radius is much larger than the heat-carrier mean free path of the host medium, which implies that the diffusive heat transport is dominant. The model shows a trend of the thermal conductivity enhancement as the particle size increases. In sum, there may be a threshold in particle size where either the Brownian motion or the diffusive heat transport is more dominant.

### 3.2 Viscosity of Al<sub>2</sub>O<sub>3</sub> nanofluids

#### 3.2.1 Effect of volume concentrations on viscosity

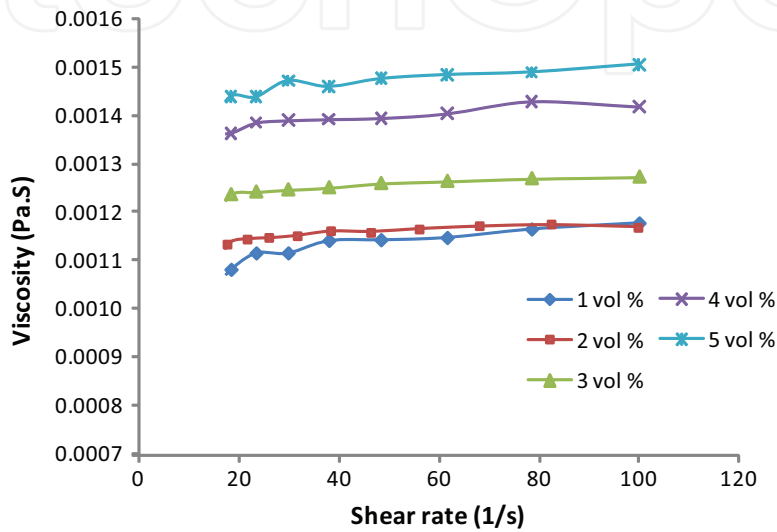


Fig. 9. Viscosity as a function of shear rate for the Al<sub>2</sub>O<sub>3</sub> nanofluids at different volume concentrations.

The viscosity is illustrated in Fig. 9 as a function of the shear rate. The viscosity of the well-mixed Al<sub>2</sub>O<sub>3</sub>-water nanofluid is independent from the shear rate. The naofluids exhibit a Newtonian behavior. Figure 10 shows that the effective viscosity ratio increases as the volume concentrations increase. The results of Masoumi et al. (2009) (28 nm) and Nguyen et al. (2007)

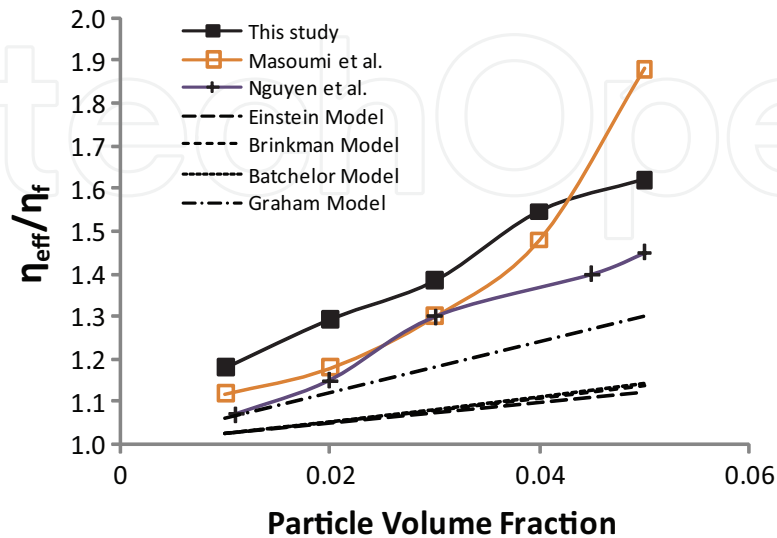


Fig. 10. Relative viscosity of the Al<sub>2</sub>O<sub>3</sub> nanofluids as a function of volume concentration.

(36 nm) show a similar trend. From our experiments, the measured viscosity of the  $\text{Al}_2\text{O}_3$  nanofluids is significantly higher than the base fluid by about 20% and 61% at 1 vol % and 5 vol % respectively. The results of Masoumi, Nguyen and ours are much higher than those of predicted values using the Einstein, Brinkman, Batchelor and Graham equations, as shown in Fig. 10. It is suggested that these equations have underestimated the nanofluid viscosities. The Einstein formula, and the others originating from it, were obtained based on the theoretical assumption of a linear fluid surrounded by the isolated particles. Such a model may work under the situation of a liquid that contains a small number of dispersed particles. However, for higher particle concentrations the departure of these formulae from our experimental data is considerable, indicating that the linear fluid theory may be no longer appropriate to represent the nanofluids. Even the Batchelor formula, considering the Brownian effect, also performs poorly. A possible explanation is mentioned by Chandrasekar et al. (2010), the large difference may be a result of the hydrodynamic interactions between particles which become important at higher volume concentrations. Hence the conventional models cannot explain the high viscosity ratio. Noted that there are also discrepancies between our experimental results and the previous studies in Fig. 10. Although the nanofluids prepared have slight differences in the size of particles, it is inappropriate to account for such a large difference in the viscosity ratio. It is difficult to draw any conclusive remarks for such results, unless this intriguing behavior may be attributed to the various factors such as nanofluid preparation methods and how the experiment is conducted.

### 3.2.2 Effect of temperature on viscosity

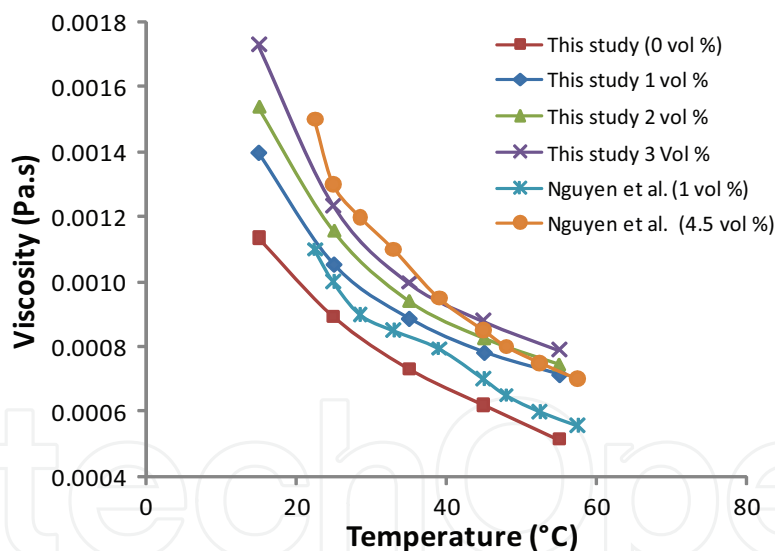


Fig. 11. Viscosity as a function of temperature for  $\text{Al}_2\text{O}_3$  nanofluids.

The viscosities were measured for the nanofluids as a function of temperature. The viscosity under the particle volume fraction ranging at 1% , 2%, and 3% from 15 to 55 °C is shown in Fig. 11, the nanofluid viscosity decreases with an increase in temperature. The increasing temperature would weaken the inter-particle and inter-molecular adhesion forces. For all the nanofluids measured, the temperature gradient of viscosity is generally steeper at the temperature from 15 to 30 °C. Such the viscosity gradient is particularly more pronounced as the particle volume concentration increases. This observation is supported by Nguyen et al. (2007) results if we compare the gradient from 15 to 30 °C at 1 vol % and 4.5 vol %. The results suggest that the temperature effect on the particle suspension properties may be

different for high particle fractions and for low ones. With an increase of temperature, the measured viscosity data have shown a gentle decrease with an increase of temperature. In our experiments, we have attempted to measure viscosity at the temperature higher than 55 °C, but a critical temperature has been observed, above the temperature, an ‘erratic’ increase of nanofluid viscosity was observed. The phenomenon may be resulted from the fast evaporation of nanofluids in the related small volume at a relative high temperature. Another possibility is that beyond the critical temperature, the surfactant might be broken down and accordingly the performance was considerably reduced or even destroyed, affecting the suspension capabilities. Thus, the particles have a tendency to form aggregation, resulting in the observed unpredictable increase of the nanofluid viscosity.

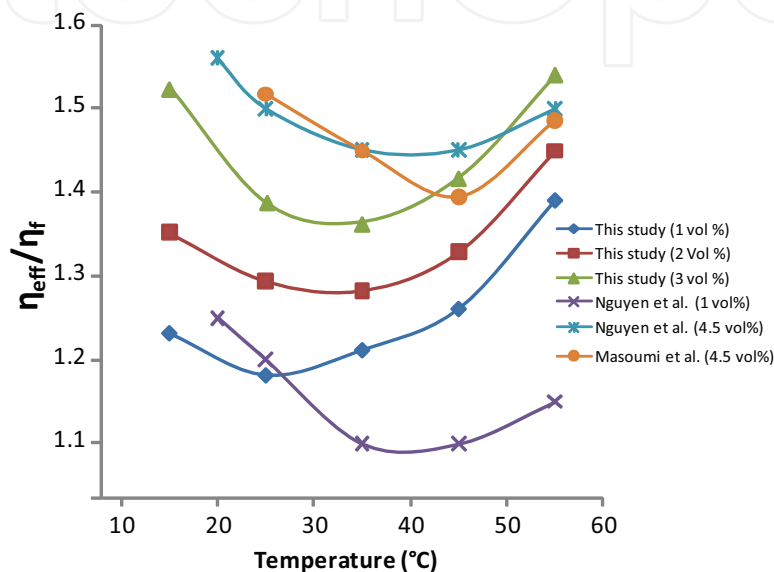


Fig. 12. Relative viscosity as a function of temperature for various concentrations of the Al<sub>2</sub>O<sub>3</sub>-water nanofluids.

As known, the water viscosity decreases with an increase of temperature. The viscosity values of the different concentration nanofluids measured from 15 to 55 °C are compared with a reference of the viscosity of water at these temperatures. As seen from Fig. 12, the effective viscosity under the different volume concentrations shows similar trends. For a given nanofluid and a particle fraction, the effective viscosity decreases at first and starts to increase at a certain temperature. This value implies that there should be an optimum temperature whereby when temperature increases, the decrease in viscosity is not effective. This observation can be substantiated by Nguyen et al. (2007) and Masoumi et al. (2009).

### 3.2.3 Effect of particle size on viscosity

From Fig. 13, our experimental results show that as the particle sizes increase, the effective viscosity decreases significantly and reaches an almost constant value at the end. This trend is similar to the results of other researchers shown in Fig. 13 except for particle size greater than 100 nm. Timofeeva et al. (2007) suggested the small particle size can form larger aggregates. The Krieger model (Krieger & Dougherty, 1959) can be used to estimate the relative viscosity between a nanofluid ( $\eta_{nf}$ ) and its base fluid ( $\eta_f$ ),

$$\frac{\eta_{nf}}{\eta_f} = \left(1 - \frac{\phi_a}{\phi_m}\right)^{-2.5\phi_m} \quad (4)$$



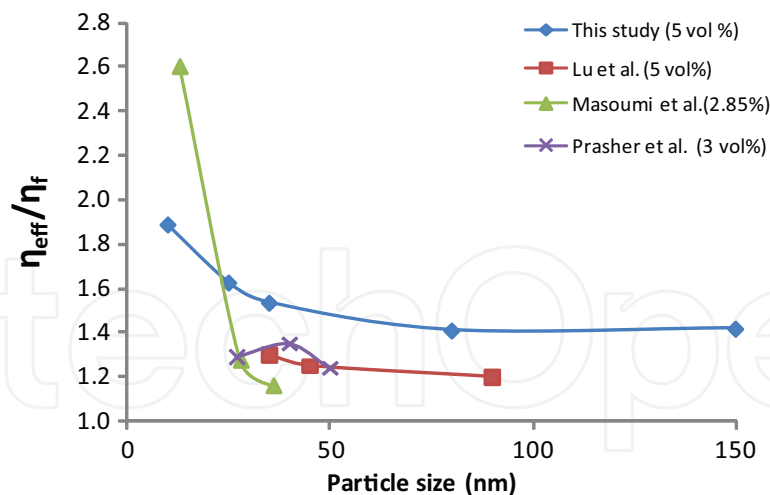


Fig. 13. Relative viscosity as a function of diameter of the  $\text{Al}_2\text{O}_3$  nanoparticles in the base fluids.

where 2.5 is the intrinsic viscosity of spherical particles,  $\phi_a$  is the volume fraction of aggregates,  $\phi_m$  is the volume fraction of densely packed spheres and the volume fraction of aggregates is expressed as  $\phi_a = \phi \left(\frac{d_a}{d}\right)^{3-d_f}$ , in which  $d_a$  is the diameter of aggregates,  $d$  is the nominal diameter of particle,  $d_f$  is the fractal dimension of the aggregates,  $\phi$  is the volume fraction of the well-dispersed individual particles. For well-dispersed individual particles,  $\phi_a$  is equal to  $\phi$ , and the Krieger model reduces to the Einstein model. This is a very ideal case where there is zero aggregation. However, none of the researches is able to obey fully the Einstein model until now. The reason may be that it is unlikely to eliminate the aggregation completely (Duan et al., 2011). When nanoparticle size increases, the magnitude of  $\frac{d_a}{d}$  decreases, thus the volume fraction of the aggregates decreases and relative viscosity ratio decreases. In addition, due to aggregation, the shape of the aggregate is no longer spherical. Theoretically, Einstein obtained the intrinsic viscosity at 2.5 for spherical particles, however the intrinsic viscosity would be greater than 2.5 for the other shapes (Rubio-hernandez et al., 2006) as the aggregate shape becomes disordered. This can also account for the increase of viscosity ratio as the particle diameter decreases.

Slight aggregation is likely to remain in our nanofluids measured just after preparation since the measurements are made for different particle sizes at a constant 5 % volume concentration, which is considered high. Based on Equation (4), the viscosity ratio would be higher after aggregation.

### 3.3 Surface tension measurements of nanofluid

Figure 14 shows the surface tension as a function of the volume concentration. The results demonstrate that the surface tensions of the  $\text{Al}_2\text{O}_3$  water-based nanofluids are significantly lower than those of the base fluid, pure water. At each point, the error bars are too small to be observed. However, as the volume concentration increases, the surface tension remains almost unchanged in the  $\text{Al}_2\text{O}_3$  nanofluids. Hence we can deduce that particle volume concentration does not have a major effect on the surface tension of the nanofluids. The experimental results of Golubovic et al. (2009) and Kim et al. (2007) have shown that the surface tensions of the  $\text{Al}_2\text{O}_3$  nanofluids without surfactant is independent on concentration and has the same values as that of pure water. In our prepared nanofluids, the surfactant, CTAB was added to obtain

a well-dispersed suspension. The addition of a small amount of surfactant into the liquid reduced the surface tension (Binks, 2002; Bresme & Faraudo, 2007).

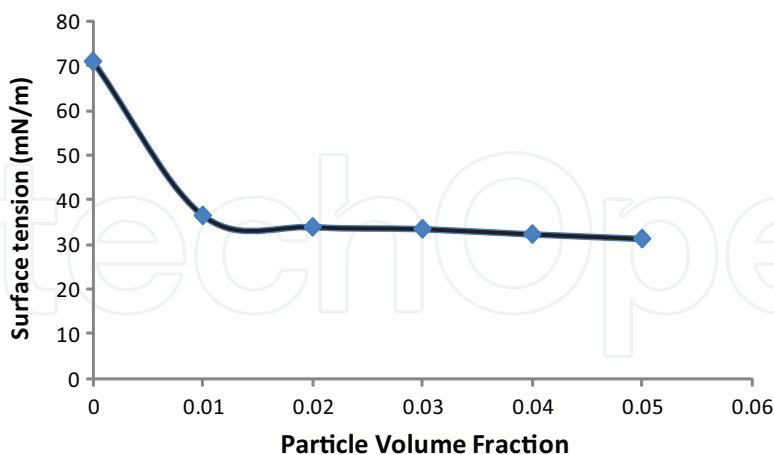


Fig. 14. Surface tension measurement of the Al<sub>2</sub>O<sub>3</sub> nanofluids as a function of the volume concentration.

#### 4. Conclusion

The thermal conductivity, viscosity, and surface tension of the Al<sub>2</sub>O<sub>3</sub> water-based nanofluids were measured. It is found the thermal conductivity increases significantly with the nanoparticle volume fraction. With an increase of temperature, the thermal conductivity increases for a certain volume concentration of nanofluids, but the viscosity decreases. The size of nanoparticle also influences the thermal conductivity of nanofluids. It is indicated that existing classical models cannot explain the observed enhanced thermal conductivity in the nanofluids. Similarly, the viscosity increases as the concentration increases at room temperature. At the volume concentrations of 5%, the viscosity has an increment of 60%. The effect of particle sizes on the viscosity is limited. The addition of surfactant is believed to be the reason behind the decrease in surface tension in comparison with the base fluid. The significant deviation between the experimental results and the existing theoretical models is still unaccounted for. More comprehensive models therefore need to be developed. Particles sizes, particle dispersions, clustering, and temperature should be taken into account in the model development for nanofluids. Hence, to reach universal models for the thermal properties, more complete experiments involving a wide range of nanoparticle sizes would be conducted in future.

#### 5. Acknowledgments

The research mainly depends on the experimental work of Mr. D. Kwok under the support of NTU-SUG and AcRF Tier 1 funding. The author would like to thank Profs. Kai Choong Leong and Charles Yang for their generosity in sharing their HWT and surface tension equipment. The author would also like thank to Dr. Liwen Jin for sharing his knowledge on the thermal conductivity measurement.

#### 6. References

Batchelor, G.K. (1977). The effect of Brownian motion on the bulk stress in the suspension of spherical particles. *J. Fluid Mech.*, 83, 97-117.

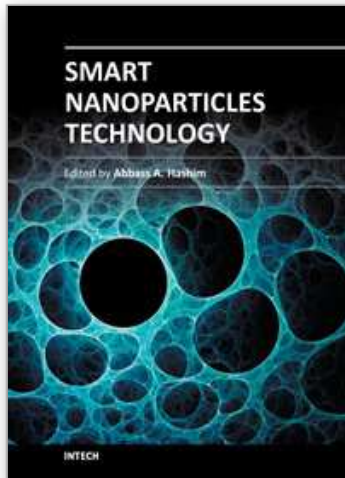
- Beck, M.P.; Yuan, Y.; Warriar, P. & Teja, A.S. (2009). The effect of particle size on the thermal conductivity of alumina nanofluids. *J. Nanopart. Res.*, 11, 1129-1136.
- Bruggeman, D.A.G. (1935). Calculation of various physics constants in heterogenous substances. I. Dielectricity constants and conductivity of mixed bodies from isotropic substances. *Ann. Phys. (Paris)*, 24, 636-664.
- Bentley, J.P. (1984). Temperature sensor characteristics and measurement system design. *J. Phys. E*, 17, 430-439.
- Bhattacharya, P.; Saha, S.K.; Yadav, A.; Phelan, P.E. & Prasher, R.S. (2004). Brownian dynamics simulation to determine the effective thermal conductivity of nanofluids. *J. Appl. Phys.*, 95, 6492-6494.
- Binks, B. (2002). Particles as surfactants - similarities and differences. *Curr. Opin. Colloid Interface Sci.*, 7, 21-41.
- Bresme, F. & Faraudo, J. (2007). Particles as surfactants - similarities and differences. *J. Phys.: Condens. Matter*, 19, 375110.
- Brinkman, H.C. (1952). The viscosity of concentrated suspensions and solution. *J. Chem. Phys.*, 20, 571.
- Chandrasekar, M.; Suresh, S. & Chandra Bose, A. (2010). Experimental investigations and theoretical determination of thermal conductivity and viscosity of Al<sub>2</sub>O<sub>3</sub>/water nanofluid. *Exp. Therm. Fluid Sci.*, 34, 210-216.
- Challoner, A.R. & Powell, R.W. (1956). Thermal conductivity of liquids: new determinations for seven liquids and appraisal of existing values. *Proc. R. Soc. Lond.*, 238, 90-106.
- Chen, G. (1996). Nonlocal and nonequilibrium heat conduction in the vicinity of nanoparticles. *ASME J. Heat Transfer*, 118, 539-545.
- Choi, S.U.S. (1995). Enhancing thermal conductivity of fluids with nanoparticles, In: *Developments and Applications of Non-Newtonian Flows*, Sinfiner, D.A. & Wang, H.P., PP 99-105, ASME, FED-vol.231 MD-vol.66, USA.
- Chon, C.H.; Kihm, K.D.; Lee, S.P. & Choi, S.U.S. (2005). Empirical correlation finding the role of temperature and particle size for nanofluid (Al<sub>2</sub>O<sub>3</sub>) thermal conductivity enhancement. *Appl. Phys. Lett.*, 87, 1-3.
- Czarnetzki, W. & Roetzel W. (1995). Temperature oscillation techniques for simultaneous measurement of thermal diffusivity and conductivity. *Int. J. Thermophys.*, 16, 413-422.
- Das, S.K.; Putta, N.; Thiesen, P. & Roetzel W. (2003). Temperature dependence of thermal conductivity enhancement for nanofluids. *J. Heat Transfer*, 125, 567-574.
- Duan, F; Kwek D & Crivoi A. (2011). Viscosity affected by nanoparticle aggregation in Al<sub>2</sub>O<sub>3</sub>-water nanofluids. *Nanoscale Res. Lett.*, 6, 248.
- Eastman, J.A.; Choi, S.U.S.; Li, S.; Thompson, L.J. & Lee, S. (1997). Enhanced thermal conductivity through the development of nanofluids. *Mater. Res. Soc. Symp. Proc.*, 457, 3-11.
- Eastman, J.A.; Choi, S.U.S.; Li, S.; Yu, W. & Thompson, L.J. (2001). Anomalously increased effective thermal conductivities of ethylene glycol-based nanofluids containing copper nanoparticles. *Appl. Phys. Lett.*, 78, 718-720.
- Einstein, A. (1906). A new determination of the molecular dimensions. *Ann. Phys.*, 19, 289-306.
- Frankel, N.A. & Acrivos, A. (1967). On the viscosity of a concentrated suspension of solid spheres. *Chem. Eng. Sci.*, 22, 847-853.
- Golubovic, M.N.; Madhawa Hettiarachchi, H.D.; Worek, W.M. & Minkowycz, W.J. (2009). Nanofluids and critical heat flux, experimental and analytical study. *Appl. Therm. Eng.*, 29, 1281-1288.
- Graham, A.L. (1981). On the viscosity of suspension of solid spheres. *Appl. Sci. Res.*, 37, 275-286.

- Hamilton, R.L. & Crosser, O.K. (1962). Thermal conductivity of heterogeneous two component systems. *Ind. Eng. Chem. Fundam.*, 1, 187-191.
- Jang, S.P. & Choi, S.U.S. (2004). Role of Brownian motion in the enhanced thermal conductivity of nanofluids. *Appl. Phys. Lett.*, 84, 4316-4318.
- Kebllinski, P.; Eastman, J.A. & Cahill, D.G. (2005). Nanofluids for thermal transport. *Mater Today*, 8, 36-44.
- Kebllinski, P.; Phillpot, S.R.; Choi, S.U.S. & Eastman, J.A. (2002). Mechanisms of heat flow in suspensions of nano-sized particles (nanofluids). *Int. J. Heat Mass Transfer*, 45, 855-863.
- Kestin, J. & Wakeham W.A. (1978). A contribution to the theory of the transient hot-wire technique for thermal conductivity measurements. *Physica A*, 92, 102-116.
- Kim, J.; Kang, Y.T. & Choi, C.K. (2004). Analysis of convective instability and heat transfer characteristics of nanofluids. *Phys. Fluids*, 16, 2395-2401.
- Kim, S.J.; Bang, I.C.; Buongiorno, J. & Hu, L.W. (2007). Surface wettability change during pool boiling of nanofluids and its effect on critical heat flux. *Int. J. Heat Mass Transfer*, 50 (2007) 4105-4116.
- Koo, J. & Kleinstreuer, C. (2004). A new thermal conductivity model for nanofluids. *J. Nanopart. Res.*, 6, 577-588.
- Krieger, I.M. & Dougherty, T.J. (1959). A mechanism for non-newtonian flow in suspensions of rigid spheres. *Trans. Soc. Rheology*, 3, 137-152.
- Kumar, D.H. Patel, H.E.; Kumar, V.R.R.; Sundararajan, T.; Pradeep, T. & Das, S.K. (2004). Model for heat conduction in nanofluids. *Phys. Rev. Lett.*, 93, 1-4.
- Kumar, R. & Milanova, D. (2009). Effect of surface tension on nanotube nanofluids. *Appl. Phys. Lett.*, 94, 073107.
- Kwek, D.; Crivoi, A. & Duan, F. (2010). Effects of temperature and particle size on the thermal property measurements of Al<sub>2</sub>O<sub>3</sub>-water nanofluids. *J. Chem. Eng. Data*, 55, 5690-5695.
- Lee, S.; Choi, S.U.S.; Li, S. & Eastman, J.A. (1999). Measuring thermal conductivity of fluids containing oxide nanoparticles. *J. Heat Transfer*, 121, 280-289.
- Li, C.H. & Peterson G.P. (2006). Experimental investigation of temperature and volume fraction variations on the effective thermal conductivity of nanoparticle suspensions (nanofluids). *J. Appl. Phys.*, 99, 1-8.
- Li, X.; Zhu, D. & Wang X. (2007). Evaluation on dispersion behaviour of the aqueous copper nano-suspensions. *J. Colloid Interface Sci.*, 310, 456-463.
- Li, Y.; Zhou J.; Tung, S.; Schneider, E. & Xi, S. (2009). A review on development of nanofluid preparation and characterization. *Powder Technol.*, 196, 89-101.
- Lundgren, T.S. (1972). Slow flow through stationary random beds and suspensions of spheres. *J. Fluid Mech.*, 51, 273-299.
- Maxwell, J.C. (1892). *A Treatise on Electricity and Magnetism*, 3rd ed., Oxford University Press, London.
- Mandelbrot; B.B. (1982). *The Fractal Geometry of Nature*, W.H. Freeman Press, San Francisco.
- Masoumi, N.; Sohrabi, N. & Behzadmehr, A. (2009). A new model for calculating the effective viscosity of nanofluids. *J. Phys. D: Appl. Phys.*, 42, 055501.
- Nagasaka, Y. & Nagashima A. (1981). Absolute measurement of the thermal conductivity of electrically conducting liquids by the transient hot-wire method. *J. Phys. E*, 14, 1435-1440.
- Nguyen, C.T.; Desgranges, F.; Roy, G.; Galanis, N.; Mare, T.; Boucher, S. & Angue Mintsa, H. (2007). Temperature and particle-size dependent viscosity data for water-based nanofluids - hysteresis phenomenon. *Int. J. Heat Fluid Flow*, 28, 1492-1506.



- Pantzali, M.N.; Kanaris, A.G.; Antoniadis, K.D.; Mouza, A.A. & Paras, S.V. (2009). Effect of nanofluids on the performance of a miniature plate heat exchanger with modulated surface. *Int. J. Heat Fluid Flow*, 30, 691-699.
- Prasher, R.; Bhattacharya, P.; Phelan, P.E. & Das, S.K. (2005). Thermal conductivity of nanoscale colloidal solutions (nanofluids). *Phys. Rev. Lett.*, 94, 025901.
- Roetzel, W.; Prinzen, S. & Xuan Y. (1990). Measurement of thermal diffusivity using temperature oscillations, In: *Measurement of conductivity 21*, Cremers C.J. & Fine, H.A., Ed., 201-207, Plenum Press, New York.
- Rubio-hernandez, F.J.; Ayucar-Rubio, M.F.; Velazquez-Navarro J.F. & Galindo-Rosales, F.J. (2006). Intrinsic viscosity of SiO<sub>2</sub>, Al<sub>2</sub>O<sub>3</sub> and TiO<sub>2</sub> aqueous suspensions. *J. Colloid Interface Sci.*, 298, 967-972.
- Sakamoto, M.; Kanda, Y.; Miyahara, M. & Higashitani, K. (2002). Origin of long-range attractive force between surfaces hydrophobized by surfactant adsorption. *Langmuir*, 18, 5713-5719.
- Schwartz, L.; Garboczi, E. & Bentz, D. (1995). Interfacial transport in porous media: application to dc electrical conductivity of mortars. *J. Appl. Phys.*, 78, 5898-5908.
- Timofeeva, E.V.; Gavrilov, A.N.; McCloskey, J.M. & Tolmachev, Y.V. (2007). Thermal conductivity and particle agglomeration in alumina nanofluids: Experiment and theory. *Phys. Rev. E*, 76, 061203.
- Vafaei, S.; Purkayastha, A.; Jain, A.; Ramanath, G. & Borca-Tasciuc, T. (2009). The effect of nanoparticles on the liquid-gas surface tension of Bi<sub>2</sub>Te<sub>3</sub> nanofluids. *Nanotechnology*, 20, 185702.
- Vargaftik, N.B.; Volkov, B.N. & Voljak, L.D. (1983). International tables of the surface tension of water. *Phys. Chem. Ref. Data*, 12, 817.
- Wang, B.X. Zhou, L.P. & Peng, X.F. (2003). A fractal model for predicting the effective thermal conductivity of liquid with suspension of nanoparticles. *Int. J. Heat Mass Transfer*, 46, 2665-2672.
- Wang, X.; Xu, X. & Choi, S.U.S. (1999). Thermal conductivity of nanoparticle - fluid mixture. *J. Thermophys. Heat Tr.*, 13, 474-480.
- Wasan, D.T. & Nikolov, A.D. (2003). Spreading of nanofluids on solids. *Nature*, 423, 156-159.
- Xie, H.; Fujii, M. & Zhang, X. (2005). Effect of interfacial nanolayer on the effective thermal conductivity of nanoparticle-fluid mixture. *Int. J. Heat Mass Transfer*, 48, 2926-2932.
- Xuan Y. & Li, Q. (2000). Heat transfer enhancement of nanofluids. *Int. J. Heat Fluid Flow*, 21, 58-64.
- Xuan, Y.; Li, Q. & Hu, W. (2003). Aggregation structure and thermal conductivity of nanofluids. *AIChE J.*, 49, 1038-1043.
- Xue, Q. (2003). Model for effective thermal conductivity of nanofluids. *Phys. Lett. A*, 307, 313-317.
- Xue, Q. & Xu, W.-M. (2005). A model of thermal conductivity of nanofluids with interfacial shells. *Mater. Chem. Phys.*, 90, 298-301.
- Yang, B. & Han, Z.H. (2006). Temperature-dependent thermal conductivity of nanorod based nanofluids. *Appl. Phys. Lett.*, 89, 1-3.
- Yu, W. & Choi, S.U.S. (2003). The role of interfacial layers in the enhanced thermal conductivity of nanofluids: a renovated Maxwell model. *J. Nanopart. Res.*, 5, 167-171.
- Yu, W. & Choi, S.U.S. (2004). The role of interfacial layers in the enhanced thermal conductivity of nanofluids: a renovated Hamilton-Crosser model. *J. Nanopart. Res.*, 6, 355-361.





## **Smart Nanoparticles Technology**

Edited by Dr. Abbass Hashim

ISBN 978-953-51-0500-8

Hard cover, 576 pages

**Publisher** InTech

**Published online** 18, April, 2012

**Published in print edition** April, 2012

In the last few years, Nanoparticles and their applications dramatically diverted science in the direction of brand new philosophy. The properties of many conventional materials changed when formed from nanoparticles. Nanoparticles have a greater surface area per weight than larger particles which causes them to be more reactive and effective than other molecules. In this book, we (InTech publisher, editor and authors) have invested a lot of effort to include 25 most advanced technology chapters. The book is organised into three well-heelled parts. We would like to invite all Nanotechnology scientists to read and share the knowledge and contents of this book.

### **How to reference**

In order to correctly reference this scholarly work, feel free to copy and paste the following:

Fei Duan (2012). Thermal Property Measurement of Al<sub>2</sub>O<sub>3</sub>-Water Nanofluids, Smart Nanoparticles Technology, Dr. Abbass Hashim (Ed.), ISBN: 978-953-51-0500-8, InTech, Available from: <http://www.intechopen.com/books/smart-nanoparticles-technology/thermal-property-measurement-of-al2o3-water-nanofluid>

**INTECH**  
open science | open minds

### **InTech Europe**

University Campus STeP Ri  
Slavka Krautzeka 83/A  
51000 Rijeka, Croatia  
Phone: +385 (51) 770 447  
Fax: +385 (51) 686 166  
[www.intechopen.com](http://www.intechopen.com)

### **InTech China**

Unit 405, Office Block, Hotel Equatorial Shanghai  
No.65, Yan An Road (West), Shanghai, 200040, China  
中国上海市延安西路65号上海国际贵都大饭店办公楼405单元  
Phone: +86-21-62489820  
Fax: +86-21-62489821

© 2012 The Author(s). Licensee IntechOpen. This is an open access article distributed under the terms of the [Creative Commons Attribution 3.0 License](#), which permits unrestricted use, distribution, and reproduction in any medium, provided the original work is properly cited.

IntechOpen

IntechOpen